

Experimental Study of the Polarization of Antiprotons from Low-Energy \bar{p} - p Elastic Scattering*

MARIO CESCHIA

Trieste University, Trieste, Italy

(Received 22 May 1969; revised manuscript received 4 February 1970)

The polarization of elastically scattered antiprotons in hydrogen, averaged with respect to the energy over the range 49.4–181.0 MeV, is evaluated as a function of the c.m. scattering angle between 16° and 100° . The result is based on an analysis of approximately 50 000 pictures taken in the 81-cm Saclay hydrogen bubble chamber, which was exposed to a separated beam from the CERN proton synchrotron. The events used for measuring the polarization were double elastic scatterings of antiprotons. The resulting polarization appears to be rather strong, and does not agree with the predictions given by the current theoretical models.

I. INTRODUCTION

THE average value, with respect to energy, of the polarization of low-energy elastically scattered antiprotons in hydrogen has been measured as a function of the scattering angle. This work completes an experimental study of the interactions of antiprotons, within a range of energy from about 50 to 190 MeV in the 81-cm Saclay hydrogen bubble chamber. The total, the differential elastic, and the charge-exchange cross sections have already been reported in previous papers.¹⁻³

About 50 000 pictures were taken during three exposures of the bubble chamber to a separated beam of antiprotons from the CERN proton synchrotron. Exposure conditions and energy determination of the beam at the entrance to the chamber (125, 156, and 190 MeV) are described in Refs. 1 and 4.

Of the 1375 events found in scanning (where the antiproton was twice scattered), only 498 were accepted for measurement. The following conditions were established for selecting the events: (a) The first and second vertex had to be contained in a suitable fiducial volume; (b) the energy of the antiproton for the first and second scattering had to fall between 49.4 and 181.0 MeV; (c) the first and second scattering of the antiproton had to give an angle between 8° and 50° in laboratory.

No measurements for low energies of the polarization of antiprotons have so far been published. Regarding higher energies, let us mention the measurement by Button and Maglič with an antiproton beam of 1.61 BeV/c momentum in the 72-in. hydrogen bubble chamber at the University of California Radiation

Laboratory⁵ and the more recent one of Dobrzynski *et al.*⁶ with antiprotons of 1.18 BeV/c in the same bubble chamber as that used for our experiment. Their results were, respectively, $e = (+25 \pm 10)\%$ —where e represents the asymmetry—for an average value of the scattering angle $\theta_{c.m.} = 25^\circ$ and $e = (-2.3 \pm 3)\%$ for an average angle $\theta_{c.m.} = 28^\circ$. At still higher energies, we can quote the experiment of Daum *et al.*,⁷ who used the counter technique and a polarized target.

The polarization which resulted from our experiment (see Fig. 1) appears rather large, particularly for the small scattering angles. This result does not agree with the predictions of existing⁸⁻¹¹ theoretical models; with regard to the optical model developed by Elagin *et al.*,¹² no polarization data have been reported by the authors, and even their phases are not available for calculation. The preliminary results of the present work were reported at the 1966 Italian Physical Society meeting.

II. METHOD

It is well known that, after double scattering of spin- $\frac{1}{2}$ particles, the differential scattering cross section I is given by

$$I = I_0(1 + P_1 P_2 \cos\Phi), \quad (1)$$

where I_0 is the differential cross section of an unpolarized beam at the second target, P_1 and P_2 determine the polarizations which would result from the scattering of an unpolarized beam at the angle and energy values for the first and second scattering, respectively, and Φ represents the azimuthal angle between the two scattering planes. The polarizations are

* Supported by Istituto Nazionale di Fisica Nucleare, Sottosezione di Trieste.

¹ U. Amaldi, Jr., B. Conforto, G. Fidecaro, H. Steiner, G. Baroni, R. Bizzarri, P. Guidoni, V. Rossi, G. Brautti, E. Castelli, M. Ceschia, L. Chersovani, and M. Sessa, *Nuovo Cimento* **46**, 171 (1966).

² B. Conforto, G. Fidecaro, H. Steiner, R. Bizzarri, P. Guidoni, F. Marcelja, G. Brautti, E. Castelli, M. Ceschia, and M. Sessa, *Nuovo Cimento* **54A**, 441 (1968).

³ R. Bizzarri, B. Conforto, G. C. Gialanella, P. Guidoni, F. Marcelja, E. Castelli, M. Ceschia, and M. Sessa, *Nuovo Cimento* **54A**, 456 (1968).

⁴ U. Amaldi, Jr., T. Fazzini, G. Fidecaro, C. Ghesquière, M. Legros, and H. Steiner, *Nuovo Cimento* **30**, 973 (1963).

⁵ J. Button and B. Maglič, *Phys. Rev.* **127**, 1297 (1962).

⁶ L. Dobrzynski, C. Ghesquière, Ng. H. Xuong, and H. Tofte, *Phys. Letters* **23**, 614 (1966).

⁷ C. Daum, F. C. Erné, J. P. Lagnaux, J. C. Sens, M. Steuer, and F. Udo, *Nucl. Phys.* **B6**, 617 (1968).

⁸ J. S. Ball and G. F. Chew, *Phys. Rev.* **109**, 1385 (1958).

⁹ M. Ceschia and A. Perlmutter, *Nuovo Cimento* **33**, 578 (1964).

¹⁰ M. S. Spergel, *Nuovo Cimento* **47**, 410 (1967).

¹¹ R. J. N. Phillips, *Rev. Mod. Phys.* **39**, 681 (1967); R. A. Bryan and R. J. N. Phillips, *Nucl. Phys.* **B5**, 201 (1968).

¹² Ju. P. Elagin, P. E. Nemirowsky, and Yu. F. Stokov, *Phys. Letters* **7**, 352 (1963); P. E. Nemirowsky and Yu. F. Stokov, *Zh. Eksperim. i Teor. Fiz.* **46**, 1379 (1964) [*Soviet Phys. JETP* **19**, 932 (1964)].

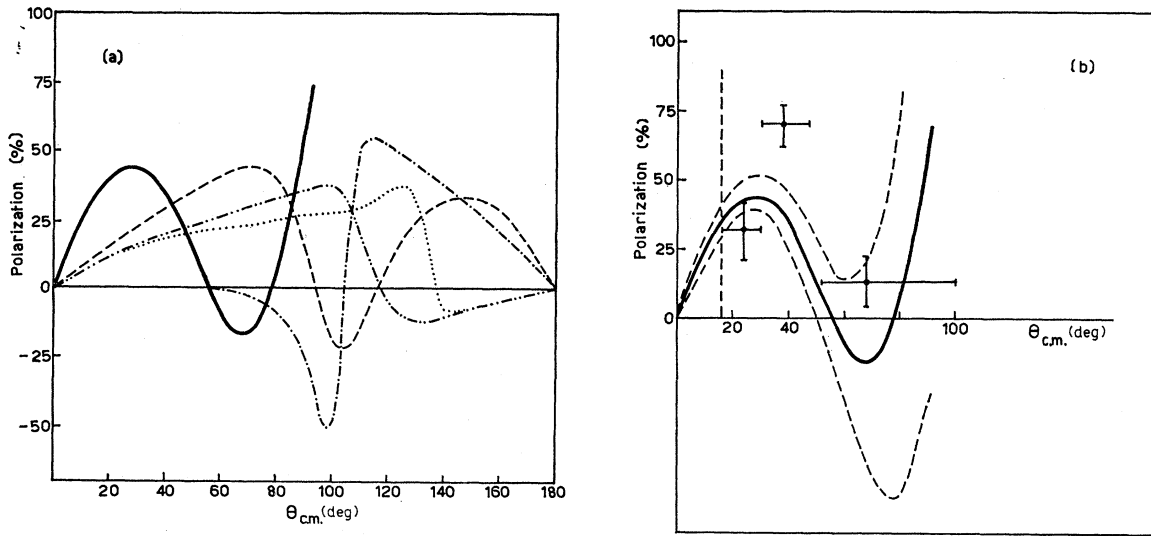


FIG. 1. (a) Comparison of experimental polarization (solid line) with theoretical predictions. Data at energies from 49.4 to 181.0 MeV. Theory: - - - Ball and Chew at 140 MeV (calculated by us, using their phases); - · - Ceschia and Perlmutter at 120 MeV; · · · Spergel at 140 MeV (best result); · · · Bryan and Phillips at 100 MeV. (b). Experimental results. The solid curve represents the average polarization; the dashed curves delimit the confidence region; the cutoff at 16° in the c.m. frame for smaller scattering angles is also indicated; the crosses represent the polarization at three angular intervals obtained by the direct procedure.

related to the asymmetry by the expression

$$e = P_1 P_2. \quad (2)$$

When experimental conditions are selected in such a way that $P_1 \approx P_2$,¹³ Eq. (2) gives, for the polarization of the antiprotons after the first scattering,

$$P_1 = \sqrt{e}. \quad (3)$$

If the two scatterings lie in the same plane, the differential cross section then becomes

$$I = I_0(1 + P_1 P_2) \quad (4)$$

and the asymmetry e can be determined by taking

$$e = \frac{(RR + LL) - (RL + LR)}{(RR + LL) + (RL + LR)}, \quad (5)$$

where RR , LL , RL , and LR denote double scattering of the type right-right, left-left, right-left, and left-right, respectively. Similarly, if the two scatterings do not lie in the same plane, we have

$$e \cos \Phi = \frac{I_0(1 + e \cos \Phi) - I_0(1 - e \cos \Phi)}{I_0(1 + e \cos \Phi) + I_0(1 - e \cos \Phi)}. \quad (6)$$

For such events, the asymmetry e can be evaluated in a more convenient way⁵ using the relation

$$e = \frac{2}{N} \sum_{i=1}^N \cos \Phi_i = P_1 P_2, \quad \text{with } \delta e = \left(\frac{2 - e^2}{N} \right)^{1/2}, \quad (7)$$

¹³ That is, double scatterings of antiproton where the first and second scattering angle are equal, and with a sufficiently small difference between the energies for the two scatterings.

where N represents the total number of events. In Eqs. (5)–(7) we disregard the effect of spin precession between the first and second scattering. To calculate the polarization using formula (7), one must obviously take into account events where the first and second scattering angles are approximately equal, thus drastically limiting available statistics.

Bearing in mind that, as far as our experiment is concerned, the energy difference between the first and second scattering appears to be somewhat large, the difficulties are considerably increased. To overcome these in part, an alternative method is to consider a particular likelihood function of the sample, written thus:

$$\begin{aligned} \mathcal{L}(a_0, a_1, a_2, \dots, a_{2L_{\max}-1}) \\ = \prod_{i=1}^N [1 + P_1(a_0, a_1, a_2, \dots, a_{2L_{\max}-1}) \\ \times P_2(a_0, a_1, a_2, \dots, a_{2L_{\max}-1}) \cos \Phi_i]. \quad (8) \end{aligned}$$

In this case each event of the sample contributes, by its own particular configuration, to the likelihood function. The polarizations P_1 and P_2 that characterize the first and second scattering can, in fact, be expressed in terms of Legendre polynomials of the order up to L_{\max} (the maximum orbital angular momentum which need be considered); thus

$$k^2 \sigma(\theta, k^2) P(\theta) = \sin \theta \sum_{l=0}^{2L_{\max}-1} a_l P_l(\cos \theta), \quad (9)$$

where, for the wave number k , the c.m. scattering angle θ , and the differential cross section $\sigma(\theta, k^2)$, we substitute

the respective values relative to the first and second scattering. The parameters which have to be determined are the coefficients of the above-mentioned expansion, i.e., $a_0, a_1, a_2, \dots, a_{2L_{\max}-1}$. As far as $\sigma(\theta, k^2)$ is concerned, we have used the experimental data quoted in Ref. 2, expressed in terms of Legendre polynomials, relative to nine energy intervals from 49.4 to 181.0 MeV. In evaluating $\cos\Phi$, we took into account the spin precession between the two scatterings resulting from the magnetic field of the bubble chamber, and for this purpose, we used the equations of Bargmann *et al.*,¹⁴ assuming the following value for the magnetic moment of the antiproton:

$$\mu_{\bar{p}} = -\mu_p = -2.79 \text{ nm}. \quad (10)$$

Under our experimental conditions the effect of the spin precession on the asymmetry appeared negligible.

Thus, to determine the polarization, we had to search for the maximum-likelihood estimates of the coefficients of its Legendre polynomial expansion. While this procedure can be considered a valid one, it depends on the assumption that the value of such coefficients remains constant. This implies that the polarization should depend on energy only through the factor $1/k^2\sigma(\theta, k^2)$, thus demanding for the different energy values in our experiment a certain similarity in its behavior versus c.m. scattering angle. Our experimental data seem to support our hypothesis (see Table I and Fig. 2). Table I gives the polarization computed for events selected, in the first case, with both scatterings at energies between 49.4 and 120.0 MeV and, in the second case, at energies between 120.0 and 181.0 MeV. The computation was carried out using formula (7). The polarization so obtained, at least for the angles under consideration (10° – 40° in laboratory), appeared more or less constant in both cases. To show that the angular dependence of the polarization is not a strong function of energy, we consider the curves of Fig. 2. These refer to events, analyzed by the likelihood method, which covered two overlapping energy intervals between 49.4 and 131.3 MeV (solid curve), and between 76.0 and 181.0 MeV (dashed curve), respectively, in both scatterings; such events had scattering angles greater than 8° in laboratory and were contained within the fiducial volume as defined in Sec. III. The limited statistics do not allow a more meaningful comparison without events in common.

A likelihood procedure, similar to that used for evaluating the polarization, enabled us also to establish the magnetic moment of the antiproton, taking into account the spin precession caused by the bubble-chamber magnetic field between the two scatterings; the magnetic moment of the antiproton thus became a parameter to be determined.

TABLE I. Results on the polarization at angles 10° – 40° (in the laboratory system) from events with both scatterings at energies contained in two intervals, 49.4–120.0 MeV, and 120.0–181.0 MeV, respectively.

Energy interval (MeV)	49.4–120.0	120.0–181.0
No. of events	170	97
Average kinetic energy at first scattering (MeV)	96	165
Average kinetic energy at second scattering (MeV)	69	138
θ_1 (av. value)	20°	18°
θ_2 (av. value)	23°	21°
Polarization (%)	45 ± 12	41 ± 17

III. STATISTICS

The film was obtained after three exposures of the 81-cm Saclay hydrogen bubble chamber to a separated beam of antiprotons. Beam and exposure details have already been described in Refs. 1 and 4. As stated in the Introduction, the energies for the three exposures at the chamber entrance—obtained by moderating the primary beam with suitable absorbers—were 125, 156, and 190 MeV, respectively. A particularly weak contamination of the beam resulted—of the order of magnitude of one pion or one muon per 10^8 antiprotons. However, taking into account the favorable exposure conditions, the antiprotons of the beam were easily distinguishable from possible contaminating mesons due to their greater specific ionization and also, since they lose more energy in the absorbers, because of their smaller curvature radius. Thus any eventual contamination of the double-scattering sample by spurious events—bearing in mind also the kinematic control—would be negligible.

We have defined a fiducial volume as being one which excludes those parts of the bubble chamber where visibility of the tracks and events is rather poor. From our

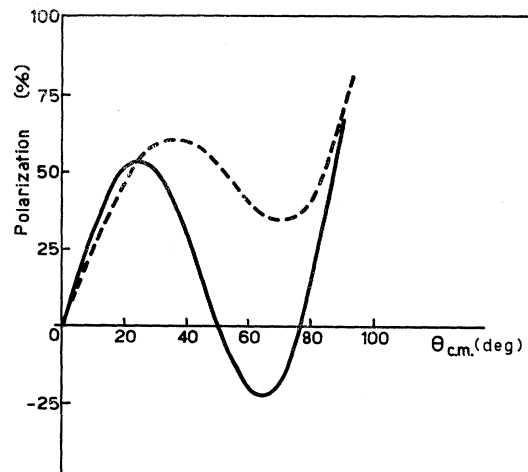


Fig. 2. Average polarization as determined from 321 events at energies 49.4–131.3 MeV (solid curve), and from 339 events at energies 76.0–181.0 MeV (dashed curve), respectively.

¹⁴ V. Bargmann, L. Michel, and V. L. Telegdi, Phys. Rev. Letters 2, 435 (1959).

sample we selected events for polarization measurement only if both vertices were inside such a volume.¹⁵ We point out, moreover, that the kinetic energies at the entrance to the fiducial volume were 121, 145, and 181 MeV for the three exposures, respectively.

The main statistics of the sample are listed below:

- (1) No. of scanned photos: 47929;
- (2) No. of double-scattering events observed at scanning: 1375;
- (3) scanning efficiency, evaluated for a single scanning on a fraction of the film: 99%;
- (4) events rejected because of having at least one scattering angle less than 8° in laboratory: 374;
- (5) events rejected as being outside the fiducial volume, but having both scattering angles greater than 8° in laboratory: 311;
- (6) among the candidates for good events (i.e., having both the scattering angles greater than 8° in laboratory and inside the fiducial volume) we had to eliminate the following: 11 rejected on scanning tables as unmeasurable, 10 THRESH rejects, 20 GRIND rejects; and
- (7) good events which were fitted to the elastic scattering of antiproton hypothesis: 649.

Particular attention was devoted to a possible polarization of the incoming beam, and using the sample of single scatterings relative to the same photos,² we measured the asymmetries e_1 and e_2 of the scattering plane about two perpendicular axes. The asymmetries were evaluated using the azimuthal distributions of the angle between the normal to the scattering plane, and an axis perpendicular to the direction of the incoming antiproton contained in the vertical plane and horizontal plane, respectively. The results are the following:

$$e_1 = (-0.3 \pm 1.4)\% \quad \text{and} \quad e_2 = (2.2 \pm 1.4)\%,$$

thus proving—if hydrogen has an analyzing power different from zero, as resulted from our experiment—that the beam is not polarized at the entrance to the bubble chamber. Similar conditions should also occur in a double-scattering sample when obtained, like ours, by random extraction from one of single scattering.

IV. RESULTS

As stated in Sec. II, there are two possible ways to evaluate the polarization: the first (more suited to our experimental conditions) by means of a particular likelihood function of the sample; the second, by following the more standard procedures introduced by Button and Maglič⁵ (used in Ref. 6). Following both procedures, we arrived at the results shown in Fig. 1. The solid curve refers to the result from an analysis using the likelihood method, taking six unknown coefficients, i.e., assuming an expansion up to $L=3$ for the polarization. The sample contained 498 events where both scattering angles were greater than 8° in laboratory, all being in-

side the fiducial volume of the bubble chamber; the events were selected in such a way as to ensure that their energy in both scatterings lies between 49.4 and 181.0 MeV.¹⁶ The average energy, computed by taking into account the energies of antiproton at both scatterings, was about 110 MeV. The coefficients which maximized the likelihood function, together with their standard errors, are

$$\begin{aligned} a_0 &= 0.41 \pm 0.05, \\ a_1 &= 0.91 \pm 0.10, \\ a_2 &= 1.20 \pm 0.13, \\ a_3 &= 1.37 \pm 0.18, \\ a_4 &= 0.83 \pm 0.15, \\ a_5 &= 0.39 \pm 0.17. \end{aligned}$$

Using these, we calculated the dashed curves¹⁷ shown in Fig. 1(b) which delimit the so-called confidence region.¹⁸ Another source of uncertainty lies in experimental errors of the cross sections used in normalizing the polarization; the effect of these errors could be such as to change the polarization level by about 10–15% for the angles covered by our experiment. To verify the magnitude of these coefficients, we have used those predicted by the Ball-Chew model⁸ at 140 MeV. The results were

$$a_0 = 0.42, \quad a_1 = 0.84, \quad a_2 = 0.78, \quad a_3 = 0.37.$$

To give some confidence in the validity of the results obtained by the likelihood method,⁵ we give below an analysis of the sample carried out by a more conventional procedure. All the events contained in the fiducial volume were subdivided into nine groups, based on selected angles for the first and second scatterings; we then drew up a matrix with their respective asymmetries, which were evaluated using the summation formula (7). Assuming the symmetry of the matrix, i.e., that the polarization did not vary with the energy, we were able to evaluate simultaneously the polarization relative to the particular angular intervals under consideration, using the least-squares technique. Figure 1(b) shows the results obtained by the subdivision which gave maximum associated probability. The relative matrix is given below.

$\theta_2 \backslash \theta_1$	$8^\circ-15^\circ$	$15^\circ-24^\circ$	$24^\circ-60^\circ$
$8^\circ-15^\circ$	0.04 ± 0.24	0.25 ± 0.17	-0.07 ± 0.17
$15^\circ-24^\circ$	0.24 ± 0.19	0.49 ± 0.15	0.19 ± 0.13
$24^\circ-60^\circ$	0.20 ± 0.22	-0.06 ± 0.17	0.02 ± 0.13

¹⁶ This allowed the polarization (expressed in terms of Legendre polynomials) to be normalized by means of the elastic differential cross section given in Ref. 2, relative to the same film.

¹⁷ Such a calculation consists in evaluating, point by point, the upper and lower boundaries enveloping all the curves which can be obtained by varying in every possible way the coefficients $a_0, a_1, a_2, a_3, a_4,$ and a_5 around their best estimates, within the standard error interval.

¹⁸ M. G. Kendall and A. Stuart, *The Advanced Theory of Statistics* (Griffin, London, 1958), Vol. II; D. J. Hudson, CERN Report No. 64-18, pp. 155–162 (unpublished).

¹⁵ Dimensions of the fiducial volume were $54.5 \times 18.0 \times 24.0$ cm³.

Here the elements are the polarization relative to i th angular interval multiplied by the polarization relative to j th; θ_1 and θ_2 are laboratory scattering angles at the first and second scattering, respectively. A comparison with the likelihood-method results shows only a qualitative agreement, but we think that it could not be improved.

From a sample of 313 events, selected in such a way that the depolarization between the two scatterings was rather large,¹⁹ we were able to obtain the following measurement of the magnetic moment of the antiproton:

$$\mu = -1.6_{-1.6}^{+1.5} \text{ (nuclear magnetons).}$$

This result was obtained using a likelihood function of the considered sample, where we had to determine the six unknown coefficients of the Legendre expansion of the polarization up to $L=3$, simultaneously with the magnetic moment of the antiproton.

V. SYSTEMATIC ERRORS

We will now examine some details of the experiment and subsequent analysis which, in our opinion, could be important in establishing the confidence level for the physical results.

In the preceding sections we have given some essential data on the beam and its degree of purity.^{1,4} The events, in which the antiprotons appeared elastically scattered twice, had already been recognized without ambiguity on the scanning table. This was due to heavy ionization of the two prongs coming from an antiproton elastic scattering in comparison with that of the annihilation prongs, as discussed in Ref. 2 for single-scattering events. The hypothesis of antiproton elastic scattering was, however, automatically verified during the kinematic analysis at both interacting vertices. We obtained, moreover, a very accurate momentum measurement from the range of the recoil proton when this was at least some millimeters in length.

The scanning losses for good events were less than 1%. However, a further 3% of good events were lost, either because they were not measurable or were THRESH rejects. For the 20 GRIND rejects, certain essential parameters were evaluated by using only their geometrical data; their contribution appeared statistically insignificant, but we verified that this did not affect the physical result.

An estimate was made of the possible effect on polarization resulting from the shape of the bubble chamber and the orientation of the magnetic field¹ which turned the antiproton tracks to the right. Here we would like

to reiterate that the events which contributed to the measurement were contained in a somewhat restricted fiducial volume, its dimensions being, in fact, $54.5 \times 18.0 \times 24.0$ cm, while those of the bubble chamber were $81 \times 30 \times 32$ cm. For each twice-elastically-scattered antiproton, we evaluated the probability (P) of its possible occurrence in the confidence volume. This probability is expressed by

$$P = 1 - \exp(-L\rho\sigma_{e1}), \quad (11)$$

where L represents the potential path length of the once-scattered antiproton inside the fiducial volume, σ_{e1} is the total elastic cross section determined at the antiproton energy corresponding to half its potential path, and ρ is the density of protons in the hydrogen of the bubble chamber. The weight W , where $W = 1/P$, evaluated for each double-scattering event, represents the number of single-scattering events²⁰ needed to observe the antiproton scattered a second time inside the fiducial volume.

We now define certain symbols which occur in the following discussion: $\cos\Phi_+$ and $\cos\Phi_-$ refer to those events for which the cosine of the angle Φ was positive and negative, respectively; L_+ and L_- refer to those events for which the first scattering was to the left, $\cos\Phi$ being positive and negative, respectively; R_+ and R_- refer to those events for which the first scattering was to the right, $\cos\Phi$ being positive and negative, respectively.

In order to find out whether the bubble chamber, on account of its particular shape, might offer symmetrical conditions for observation of events with $\cos\Phi_+$ as against those with $\cos\Phi_-$, we considered first the weight distribution for the two categories. These distributions are shown in Figs. 3(a) and 3(b), respectively. As was foreseen, the difference between the number of events with $\cos\Phi_+$ and that with $\cos\Phi_-$ appeared greater for those having weights between 9 and 20; in this latter range the events with a scattering angle of less than 30° in the laboratory were more frequent, and it was here that the polarization was, on the average, larger. From a comparative examination of the two figures, it does not seem possible to find any particular effect which would lead to easier observation of one type rather than the other. The cutoff for weights less than 8 is the same for both types; it depends on the probability that the once-scattered antiproton has of being re-scattered in the fiducial volume of the bubble chamber at its maximum attainable value under our experimental conditions. The standard conditions for observing double-scattering events of both types correspond, in our experiment, to weights between about 9 and 20; moreover, some large weights are noted in the two types. In Fig. 4 we compare the differential cross section ob-

¹⁹ That is, the events were contained within the fiducial volume and the antiproton scattering angle at first and second scattering was greater than 8° in laboratory; the track length connecting the two vertices was greater than or equal to 5 cm, and the angle between the front glass and the scattering planes was greater than or equal to 20° .

²⁰ We note that these should be events with the same potential path inside the fiducial volume and the same energy for the scattered antiproton.

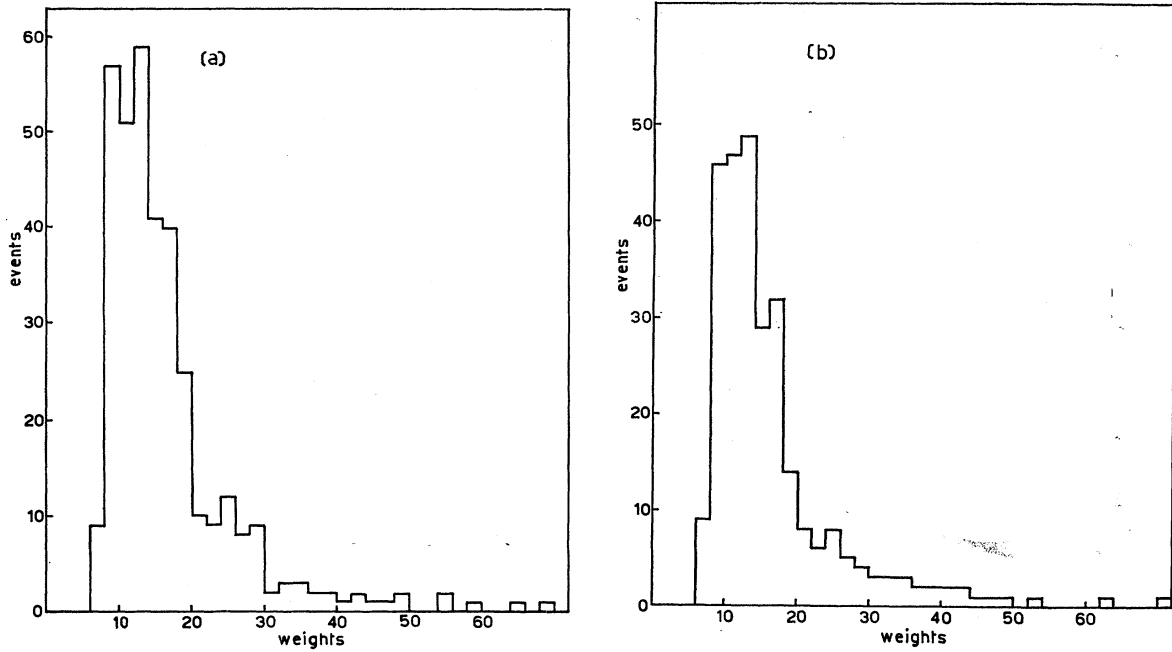


FIG. 3. Detection-weights distributions for double-scattering events (a) with $\cos\Phi_+$ and (b) with $\cos\Phi_-$.

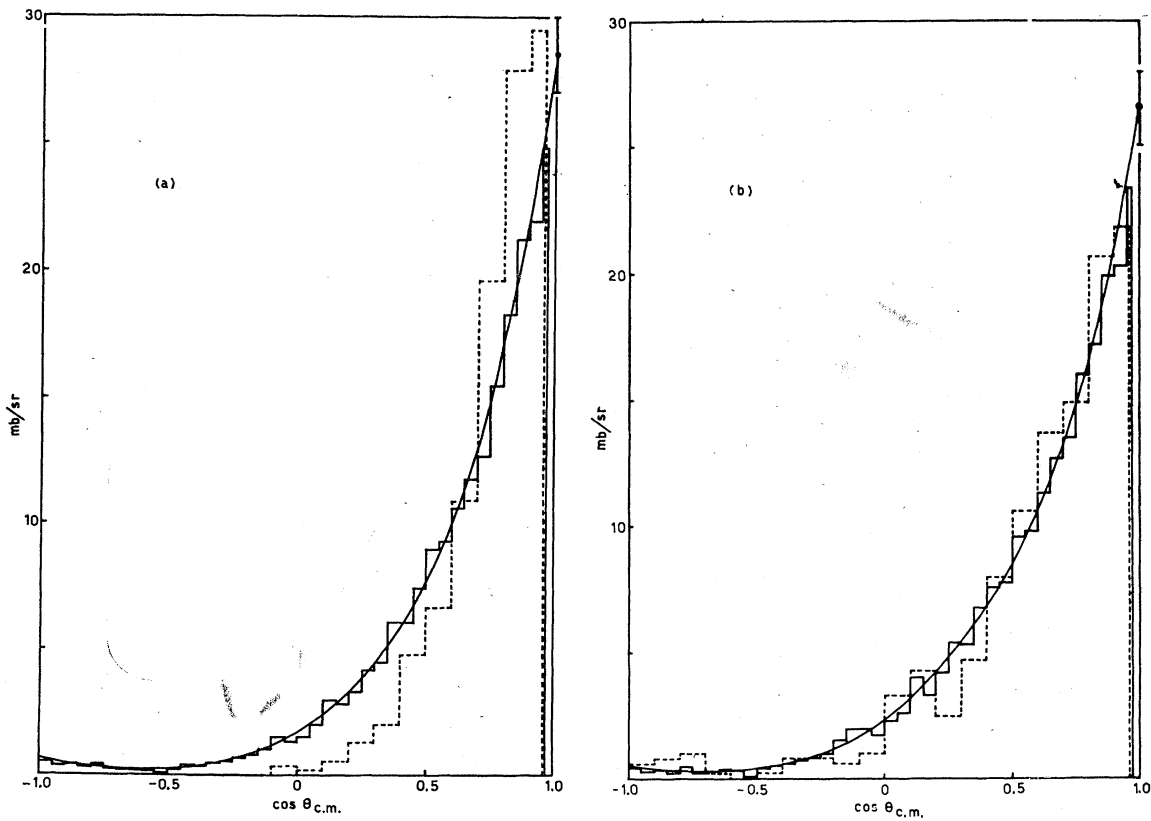


FIG. 4. Comparison between the differential cross section from the double-scattering sample (dashed line) with the cross section estimated by averaging the data in Ref. 2 for a hypothetical sample of single-scattering events having the same energy distribution (solid line) (a) at first scattering, (b) at second scattering.

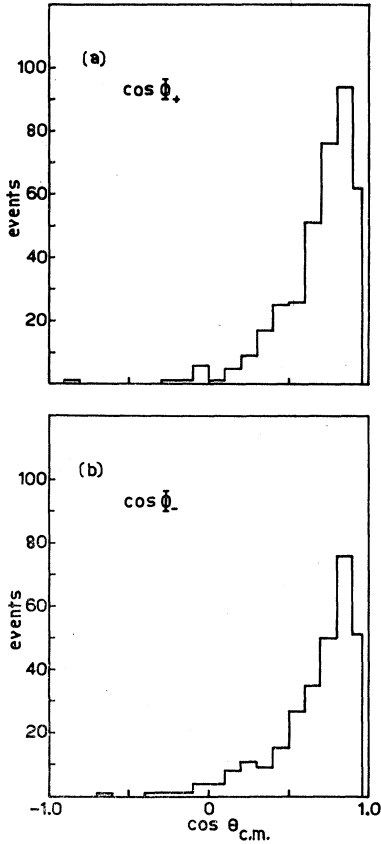


FIG. 5. Angular distributions of once-scattered antiprotons for double-scattering events (a) with $\cos\Phi_+$ and (b) with $\cos\Phi_-$.

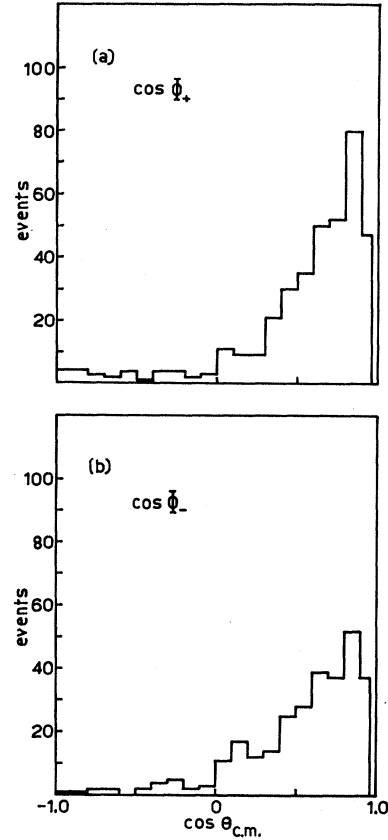


FIG. 6. Angular distributions of twice-scattered antiprotons for double-scattering events (a) with $\cos\Phi_+$ and (b) with $\cos\Phi_-$.

tained from the double-scattering sample (dashed line) with the cross section estimated by averaging the data in Ref. 2 for a hypothetical sample of single-scattering events having the same energy distribution (solid line). Figure 4(a) refers, in particular, to the first scattering while Fig. 4(b) refers to the second. The former shows clearly that the special shape of the bubble chamber strictly limits the observation of double-scattering events where the once-scattered antiproton has a c.m.

TABLE II. Data relative to the sample of good events subdivided into events classified as types L_+ , L_- , R_+ , and R_- . The same data including, whenever possible, the GRIND rejects are shown in parentheses. Note that the angles and energies are in the laboratory system.

No. of events	L_+	L_-	R_+	R_-	Total
	177	129	187	156	649
	(184)	(136)	(191)	(158)	(669)
Mean weights	17.9	18.2	17.4	16.3	
θ_1° (av.)	21.0	20.8	21.3	22.8	
	(21.6)	(21.0)	(21.7)	(22.9)	
θ_2° (av.)	27.4	28.1	24.8	25.5	
	(27.8)	(28.1)	(24.8)	(25.6)	
$E_{1\text{ av}}$ (MeV)	117	114	120	120	
$E_{2\text{ av}}$ (MeV)	84	82	88	86	

scattering angle greater than about 60° . The probability, calculated with Eq. (11), of observing such events in the fiducial volume is in fact small, this being inevitable when taking into account the shorter potential path of the antiproton. The differential cross section evaluated for the second scattering is, on the other hand, in good agreement with that for the single-scattering sample. In Figs. 5 and 6 we show the partial angular distributions, i.e., relative to double-scattering events with $\cos\Phi_+$ and $\cos\Phi_-$, for antiprotons scattered the first and second time, respectively. The partial distributions show that the observational conditions for events with $\cos\Phi_+$ as against those with $\cos\Phi_-$ were not dissimilar to those in toto. The fact that the distributions with $\cos\Phi_+$ are more populated than those with $\cos\Phi_-$ —this being more

TABLE III. Mean values for the entrance parameters of the double-scattering events in the angular interval 15° - 24° in the laboratory system. The same data for the whole sample are shown in parentheses.

No. of events	y_0 (cm)	z_0 (cm)	α (rad)	β (rad)
78	3.09	16.28	0.123	0.015
(649)	(3.30)	(16.07)	(0.131)	(0.013)

evident for those scattering angles where the polarization was greater—ought then to express an objective physical situation, namely, nonzero polarization.

Finally, to complete the search for possible effects due to the shape of the bubble chamber, we subdivided the sample of good events into events classified as types L_+ , L_- , R_+ , and R_- . Table II gives the most significant data relative to this subdivision but does not show any specific situation which could affect the physical result.

The depolarization between the first and second scattering—expressed by the angle $\delta' = \delta - \Delta$, where δ represents the spin precession, and Δ the magnetic deflection—was, in our case, small. In fact, its average value, obtained by considering the aforementioned good events (649), was

$$\delta' = 19^\circ.$$

Thus the use of the summation formula in our experi-

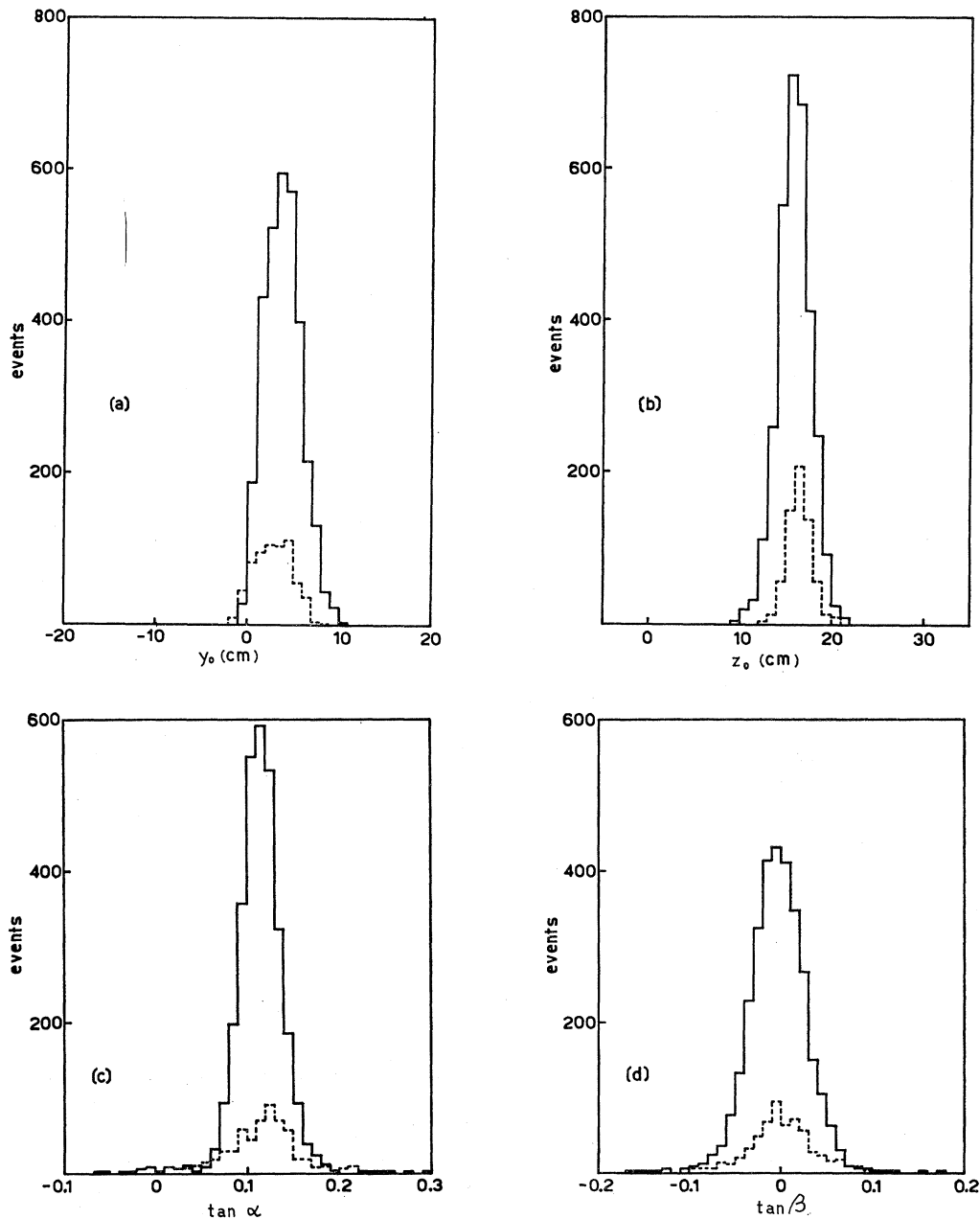


Fig. 7. Distributions of entrance parameters in the fiducial volume y_0 , z_0 , $\tan\alpha$, and $\tan\beta$ for 3005 interacting tracks in the third exposure (solid line) and 649 double-scattering events (dashed line).

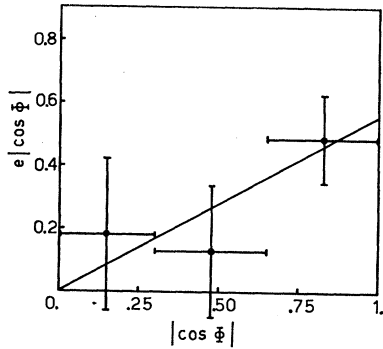


FIG. 8. The quantity $e|\cos\Phi|$ versus $|\cos\Phi|$ as determined from the good events having both laboratory scattering angles between 15° and 24° .

ment is amply justified; on the other hand, the measurement of the magnetic moment of the antiproton from the depolarization became rather difficult.

It now remains to verify the random extraction of the double-scattering sample from that of single scattering. To this end, we compared the distributions of the parameters of the beam entering the confidence volume (y_0 , z_0 , $\tan\alpha$, and $\tan\beta$) with analogous distributions for single scatterings (shown in Ref. 1 for the third exposure only). If we consider that all three exposures (with in-flight antiprotons) contributed to the sample of double-scattering events, there is no appreciable difference in the behavior of the respective distributions (see Fig 7).

Finally, we consider some details of the good events possessing both laboratory scattering angles between 15° and 24° . For these angles we obtained the largest asymmetry, which, as determined by formula (7), is already reported in Sec. IV. The value for $e|\cos\Phi|$, computed by using Eq. (6), as a function of $|\cos\Phi|$ is shown in Fig. 8; the best fit is obtained where $e=0.55$. Table III gives the mean values of the entrance parameters y_0 , z_0 , $\tan\alpha$, and $\tan\beta$, and Fig. 9 shows the energy behavior of antiprotons at the entrance to the fiducial volume with respect to the whole sample of double-scattering events.

VI. CONCLUSION

The result of this experiment can be considered as evidence for a rather strong polarization with a maxi-

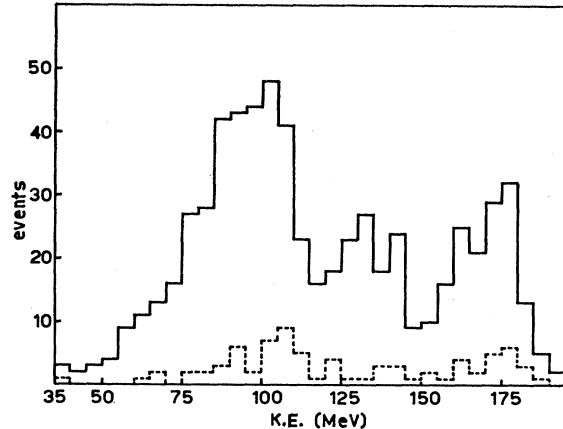


FIG. 9. Laboratory kinetic-energy distribution of antiprotons at the entrance to the fiducial volume for the whole sample of double-scattering events (solid line) and for events having the first and second scattering angle between 15° and 24° in laboratory (dashed line).

mum at about 40° in the c.m. frame for the explored angular region. This could be interpreted as a surprising result, particularly in regard to the smaller scattering angles, when referred to the present models on nucleon-antinucleon interactions. However, if we examine these models in detail, we can see that the imaginary part of the potentials is simply phenomenological; no spin or isospin dependence was taken into account. Only the real part of the potentials is well known; in fact, several details have already been verified. All the models developed up to now⁸⁻¹¹—including the one of Bryan and Phillips, which is the most advanced—have only foreseen a weak polarization at the angles involved in our experiment. To give an over-all picture, however, we have plotted in Fig. 1(a) all the theoretical data available till now, together with the results of the present work.

ACKNOWLEDGMENTS

I would like to thank all the members of the CERN-Roma-Trieste collaboration for having put at my disposal the double-scattering data; in particular I am indebted to Professor R. Bizzarri for his continual interest and criticism. Professor H. Steiner commented on some points in this work.